Carbohydrate Polymers 83 (2011) 1162–1168

Contents lists available at ScienceDirect

Carbohydrate Polymers

journal homepage: www.elsevier.com/locate/carbpol

Preparation and characterization of α-galactosidase-loaded chitosan nanoparticles for use in foods

Yong Liu[a], Yan Sun[b], Yanli Li[a], Shaochun Xu[a], Jiangwu Tang[a], Juntao Ding[b], Yaoxing Xu[a,*]

[a] Zhejiang Academy of Agricultural Sciences, Institute of Plant Protection and Microbiology, 198 Shiqiao Road, Hangzhou, Zhejiang Province 310021, China
[b] Hangzhou Normal University, Post Box 206, 222 Wenyi Road, Hangzhou, Zhejiang Province 310012, China

ARTICLE INFO

Article history:
Received 20 May 2010
Received in revised form 10 July 2010
Accepted 10 September 2010
Available online 25 October 2010

Keywords:
α-Galactosidase
Chitosan
Nanoparticles
Encapsulation

ABSTRACT

The instability of enzymes used in animal and human foods has long been an important issue in food preparation and storage. Recent breakthroughs in nanotechnology have shown the great advantages of nanoparticles (NPs) in protein encapsulation and controlled release. α-Galactosidase and chitosan (CS) were chosen as models for food enzymes and coating materials, respectively. A series of α-galactosidase-loaded CS NPs were prepared. The burst release of α-galactosidase from NPs and thermal stability of α-galactosidase after coating were tested. α-Galactosidase-loaded NPs were characterized by Fourier transform infrared (FTIR) spectroscopy, differential scanning calorimetry (DSC), transmission electron microscopy (TEM), photon correlation spectroscopy (PCS), and zeta potential analysis.

The results were as follows:

(1) α-Galactosidase was successfully encapsulated in CS NPs.
(2) α-Galactosidase-loaded CS NPs had high encapsulation efficiency.
(3) The thermal stability of α-galactosidase was significantly increased after loading with CS NPs.
(4) The burst release efficiency of CS NPs loaded with α-galactosidase was higher than 90% at pH 3.0 and 10.0.

1. Introduction

α-Galactosidase (E.C. 3.2.1.22) is a polysaccharide hydrolase that hydrolyzes both simple α-galactosides and complex polysaccharides containing α-galactosides bonds. Because of its terminal α-1,6-linked galactose residue hydrolysis activity, α-galactosidase is widely used in chick and pig feeds to degrade anti-nutritional oligosaccharides, such as melibiose, raffinose, and stachyose (Ao, Cantor, Pescatore, Ford, & Pierce, 2004; Baucells, Perez, Morales, & Gasa, 2000; Kidd et al., 2001; Kim, 2002). α-Galactosidase, however, is sensitive to pH and heat. Its activity is quickly lost in food storages at room temperature. Therefore, novel coating treatments could be helpful in improving its usage properties.

CS is produced from chitin, one of the most abundant biopolymers in nature. CS has a very diverse range of established and potential applications. The great potential of CS is generally related to its poly-cationic properties, which are unique among abundant polysaccharides and natural polymers. CS has been proven to be non-toxic, biodegradable, bio-functional, biocompatible, and antimicrobial (Jayakumara, Prabaharanb, Naira, & Tamura, 2010). Because of its favorable physicochemical and biological properties, CS is considered an attractive material that could potentially be used in many biomaterial-related applications, such as drug delivery (Janes, Calvo, & Alonso, 2001; Masotti & Ortaggi, 2009), plant protection (Bautista, Hernandez, Bosquez, & Wilson, 2003), antibacterial functions (Fu, Ji, Yuan, & Shen, 2005; Qi, Xu, Xia, Hu, & Zou, 2004), DNA biosensors (Li, Liu, Liu, Liu, & Yao, 2005), tissue engineering (Mi et al., 2001; Wang, Lin, Wang, & Hsieh, 2003), food additives (Pittler & Ernst, 2004), feed additives (Kobayashi, Terashima, & Itoh, 2002; Senel & Susan, 2004), water treatment (Amit & Mika, 2009) and food packaging (Cagri, Ustunol, & Ryser, 2004), among others.

In this work, CS was used as a feed enzyme supplementation coating material. A series of α-galactosidase-loaded CS NPs were prepared, and their physicochemical structures were analyzed by

Abbreviations: NPs, nanoparticles; CS, chitosan; TEM, transmission electron microscopy; PCS, photon correlation spectroscopy; TPP, sodium tripolyphosphate; MW, molecular weight; FTIR, Fourier transform infrared spectroscopy; DSC, differential scanning calorimetry.

* Corresponding author. Tel.: +86 571 86404254; fax: +86 571 86404254.
E-mail addresses: xuyx007@163.com, lylyhaha1978@163.com (Y. Xu).

0144-8617/$ – see front matter © 2010 Elsevier Ltd. All rights reserved.
doi:10.1016/j.carbpol.2010.09.050

FTIR, DSC, PCS, zeta potential analysis, and TEM. In addition, the release properties of α-galactosidase from α-galactosidase-loaded CS NPs were also tested at different pH levels. The major goal of this work was to create a new α-galactosidase coating system, and to evaluate its potential as a common feed enzyme supplementation coating material.

2. Materials and methods

2.1. Materials

CS samples with different MWs (50, 400, 670, and 1880 kDa; deacetylation degree, 92%) were obtained from Jinhu Co., Ltd. (China). α-Galactosidase was prepared in our lab according to Xu's method (Xu, Li, Liu, Xu, & Yao, 2009). Sodium tripolyphosphate (TPP) was obtained from Shanghai Sangon Biological Engineering Technology & Services Co., Ltd. All other chemicals were of reagent grade.

2.2. Preparation of pure CS NPs and α-galactosidase-loaded CS NPs

2.2.1. Preparation of α-galactosidase-loaded CS NPs with different concentrations and pH values of CS solution

Different concentrations of CS (1.0, 2.0 and 3.0 mg/mL) were separately dissolved in 1% acetic aqueous solution. Each CS concentration was further sampled into several flasks, with the pH of each flask adjusted to 3.0, 4.0, 4.5, 5.0, 5.5, and 6.0 by sodium hydroxide or acetic acid. A TPP solution was dropped into each CS solution under magnetic stirring. After 30 min of cross-linking, an opalescent suspension was spontaneously formed. Further examination determined that the suspension contained pure CS NPs. For another set of experiments, 2.0 mL of α-galactosidase (2.0 mg/mL, 400 IU/mL) was added into 20.0 mL of each CS solution. After thorough mixing, TPP was added to the α-galactosidase-CS solutions (CS/TPP ratio at 4/1) under room temperature and magnetic stirring. An opalescent suspension was spontaneously formed. Further examination determined that the suspension contained α-galactosidase-loaded CS NPs.

2.2.2. Preparation of α-galactosidase-loaded CS NPs with different CS/TPP ratios

CS samples (MW 50 kDa) were separately dissolved in a 1% acetic aqueous solution at concentration of 2.0 mg/mL. The pH of each sample was adjusted to 3.0, 4.0, 4.5, 5.0, 5.5, and 6.0. About 2.0 mL of the α-galactosidase solution was then added to 20.0 mL of the CS solution under room temperature and magnetic stirring. Then, 3.5 mL of a TPP solution (different concentrations, pH 5.5) was added to the α-galactosidase–CS solutions. The CS/TPP ratios were set to 3/1, 4/1, 5/1, 6/1, and 8/1. Opalescent suspensions were spontaneously formed. Further examination revealed that these suspensions contained NPs. For the control, 3.5 mL of double-distilled water was added to the α-galactosidase–CS solutions instead of TPP.

2.2.3. Preparation of α-galactosidase-loaded CS NPs with different α-galactosidase concentrations

CS (MW 50 kDa) was dissolved in 1% acetic aqueous solution at a concentration of 2.0 mg/mL, and its pH was adjusted to 5.5. A total of 20.0 mL of the α-galactosidase solution (different concentrations, pH 5.5) was added to 20.0 mL of the CS solution. The final concentrations of α-galactosidase were set to 0.125, 0.2, 0.4, 0.675, and 1.0 mg/mL. Finally, 2.5 mL of TPP (4.0 mg/mL, pH 5.5) was added to the α-galactosidase-CS solutions dropwise under room temperature and magnetic stirring. Opalescent suspensions were spontaneously formed. Further examination of the suspensions revealed that they contained NPs. For the control, 2.5 mL of double-distilled water was added to control beakers instead of TPP. The initial concentration of α-galactosidase was determined by UV spectrophotometry at 280 nm using double-distilled water as a basic correction.

2.2.4. Preparation of α-galactosidase-loaded CS NPs with different CS MWs

CS samples with different MWs (50, 400, 670, and 1880 kDa) were dissolved at the same concentration (2.0 mg/mL), and their pH levels were adjusted to 5.5. About 2.0 mL of the α-galactosidase solution was added to 20.0 mL of the CS solution. Finally, 2.0 mL of TPP (4.0 mg/mL, pH 5.5) was added to the α-galactosidase-CS solutions under room temperature and magnetic stirring. An opalescent suspension was spontaneously formed. Further examination showed that it contained NPs. For the control, 2.5 mL of double-distilled water was added to control beakers instead of TPP.

2.3. FTIR analysis

The FTIR spectra of CS, 5.5-CS-NPs (pH 5.5), 5.5-CS/α-galactosidase-NPs (α-galactosidase-loaded CS NPs at pH 5.5), and α-galactosidase were recorded. Spectra were recorded on an IR spectrometer (Model: Paragon 1000, Perkin Elmer, USA) in the range of 1000–4000 cm^{-1}. Signal averages were obtained for 32 scans at a resolution of 4 cm^{-1}.

2.4. DSC analysis

The DSC thermograms of CS, 5.5-CS-NPs (pH 5.5), 5.5-CS/α-galactosidase-NPs (α-galactosidase-loaded CS NPs at pH 5.5), and α-galactosidase were recorded on a Perkin-Elmer PYRIS I. A sample of about 2–6 mg was accurately weighed on a solid aluminium pan with a sealed cover. The measurements were performed under nitrogen at a constant heating rate of 20 °C/min. The vessel was constantly purged with nitrogen at a rate of 20.0 mL/min. All samples were run in duplicate.

2.5. Evaluation of α-galactosidase encapsulation efficiency

The encapsulation efficiency of α-galactosidase in each studied group was determined by measuring the α-galactosidase remaining in the supernatant after centrifuging the samples for 30 min at 20,000 × *g* and 15 °C. The amount of α-galactosidase in the clear supernatant was determined by enzyme activity following Irma's method (Irma, Ana, Caren, Peter, & Cees, 1992). The α-galactosidase encapsulation efficiency of the process was calculated using Eq. (1):

$$L_E = \frac{A - B}{A} \times 100 \quad (1)$$

where L_E is the α-galactosidase encapsulation efficiency, A is the total amount of α-galactosidase, and B is the free amount of α-galactosidase in the supernant.

2.6. pH-mediated burst release of α-galactosidase in vitro

α-Galactosidase-loaded CS NPs were prepared as follows: 2.0 mL of the α-galactosidase solution (2.0 mg/mL, 400 IU/mL, pH 5.5) was added to 20.0 mL of the CS solution (2.0 mg/mL, pH 5.5). About 2.5 mL of TPP (4.0 mg/mL, pH 5.5) was then dropped into the α-galactosidase-CS solution under room temperature and magnetic stirring. An opalescent suspension was spontaneously formed. Further examination showed that it contained

α-galactosidase-loaded CS NPs. This suspension was used to evaluate the vitro α-galactosidase burst release. The α-galactosidase encapsulation efficiency was calculated according to Eq. (1).

A 1.0 mL suspension of α-galactosidase-loaded CS NPs was mixed with 4.0 mL of buffer at pH 3.0, 4.0, 5.0, 6.0, 7.0, 8.0, 9.0, and 10.0. The mixtures were placed at room temperature for 10 min, after which they were centrifuged for 30 min at 20,000 × *g* and 15 °C. The free amounts of α-galactosidase in the supernatants were determined by enzyme activity according to Irma's method (Irma et al., 1992). The cumulative α-galactosidase in the supernatant was calculated using Eq. (2):

$$L_C = \frac{B}{A} \times 100 \quad (2)$$

where L_C is the cumulative percent of α-galactosidase in the supernatant, A is the total amount of α-galactosidase, and B is the free amount of α-galactosidase in the supernatant.

2.7. Evaluation of thermal stability of α-galactosidase after loading with CS NPs

A suspension of α-galactosidase-loaded CS NPs was prepared as described in Section 2.6. And 4.0 mL of the suspension was treated at a 60 °C water bath for 30 min. For the control, pure α-galactosidase of the same amount and concentration was treated similarly. The residual activity of α-galactosidase was determined using Irma's method (Irma et al., 1992).

2.8. Statistical analysis

All experiments were repeated a minimum of three times and measured in triplicate. Results reported were means ± SD, unless otherwise noted. Statistical significance was analyzed using Student's *t*-tests. Differences between experimental groups were considered significant at $p < 0.05$.

2.9. Nanoparticle characterization

The morphological measurements of the NPs were determined using TEM (JEM-100CX, JEOL, Japan). The average particle size and size distribution were determined using PCS with a Netasizer Nano S90 (Malvern Instruments Ltd., United Kingdom). The zeta potential measurements of the nanoparticles were obtained using a Zetasizer 2000 (Malvern Instruments Ltd., United Kingdom). Samples for testing were prepared as in Section 2.6.

3. Results and discussion

3.1. FTIR characterization

The FTIR spectra of CS, 5.5-CS-NPs, 5.5-CS/α-galactosidase-NPs, and α-galactosidase are shown in Fig. 1. The absorption band at 1657 cm^{-1} in native chitosan (Fig. 1A) was referenced as amide I bands, while the absorption band at 1606 cm^{-1} was ascribed to the N–H bending mode in the primary amine. The absorption band at 1606 cm^{-1} was ascribed to the N–H bending mode in the primary amine of chitosan (Fig. 1A), but it disappeared in the 5.5-CS-NPs (Fig. 1B), which could be attributed to the linkage between the tripolyphosphoric groups of TPP and the ammonium groups of CS in CS-NPs (Knaul, Hudson, & Creber, 1999). The acetylamino I at 1657 cm^{-1} in α-galactosidase (Fig. 1D) overlapped with the d (NH) in non-loaded CS NPs, so more intense peaks for both were found in the spectrum of 5.5-CS/α-galactosidase-NPs (Fig. 1C). In addition, a characteristic peak at 1565 cm^{-1}, attributed to the amide II band of the CS-TPP NPs, became weak. The results indicate that some interactions had occurred between the NH_2 groups of CS and TPP in the CS NPs. α-Galactosidase was successfully encapsulated in the CS NPs.

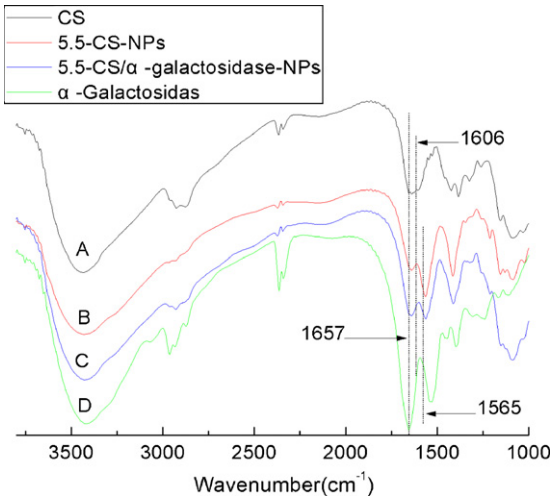

Fig. 1. FTIR spectra of CS, 5.5-CS-NPs, 5.5-CS/α-galactosidase NPs, and α-galactosidase.

3.2. DSC analysis

A DSC (Model: Perkin-Elmer PYRIS I) was used. Each sample (2–6 mg) was run at a scanning rate of 20 °C/min under a nitrogen atmosphere. The temperature for the first scan ranged from 20 to 120 °C, held for 5 min at 120 °C, and then to −30 °C at a rate of 20 °C/min. This was followed by an immediate rescanning in the range of −30 °C to 300 °C. Polysaccharides usually have a strong affinity for water, and, in the solid state, these macromolecules may have disordered structures that can be easily hydrated. As such, the first scan was used to exclude hydrated water from the NPs and eliminate its influences.

Fig. 2 shows the thermal transitions of CS, 5.5-CS-NPs, 5.5-CS/α-galactosidase-NPs, and α-galactosidase. The analysis of the DSC curves for CS (Fig. 2A) showed a small endothermic peak at an onset of 250 °C, which indicated the onset of chitosan degradation (Khalid, Agnely, Yagoubi, Grossiord, & Couarraze, 2002). In the case of pure CS, however, no clear glass transition temperature (T_g) was exhibited. The T_g of chitin and chitosan had been previously predicted to be latent in the decomposition temperature >230 °C, as in the case of cellulose (Kittur, Harish Prashanth, Udaya, & Tharanathan, 2002). In the DSC curve of α-galactosidase (Fig. 2B), an endothermic peak centered at near 190 °C was possibly linked to the decomposition of α-galactosidase. Compared to pure CS, a wide

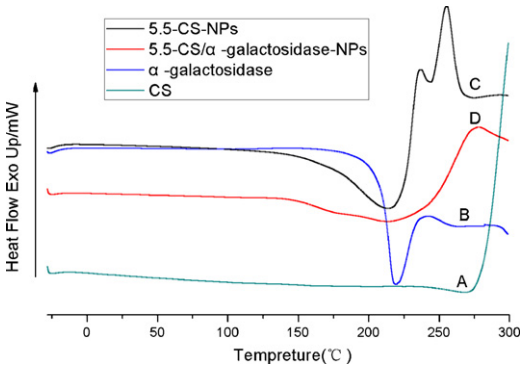

Fig. 2. DSC analysis of CS, 5.5-CS-NPs, 5.5-CS/α-galactosidase NPs, and α-galactosidase.

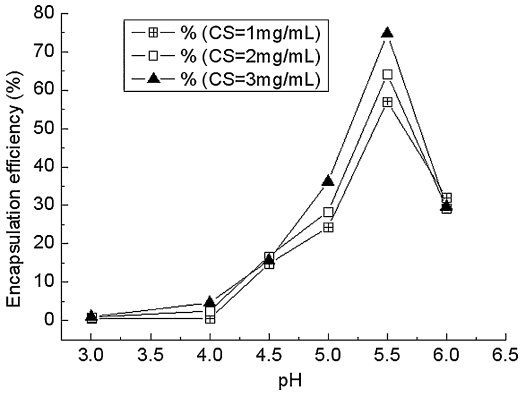

Fig. 3. Effect of CS concentrations and pH value on encapsulation efficiency.

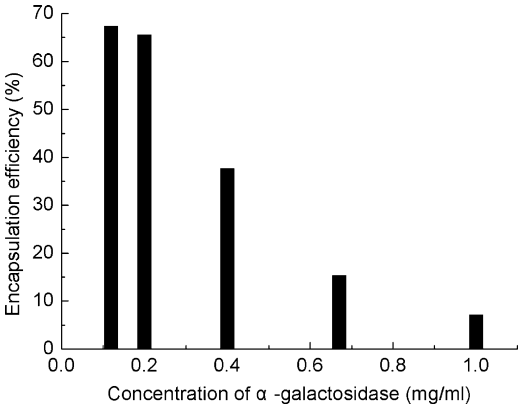

Fig. 5. Effects of α-galactosidase concentration on encapsulation efficiency.

endothermic peak centered between 200 and 220 °C, with an onset at 120 °C, appeared for the 5.5-CS-NPs (Fig. 2C), which was probably related to the breakdown of weak electrostatic interactions between TPP and CS. In addition, there appeared two significant exothermic peaks at 240 and 260 °C.

These may have appeared because TPP and CS can form weak ionic interactions with each other, and these interaction points could act as physical cross-linking points and increase chain rearrangement. Thus, the new crystal structure of CS was created. After loading α-galactosidase, 5.5-CS/α-galactosidase-NPs (Fig. 2D) had lower values of enthalpy change (ΔH), which indicates that α-galactosidase hindered electrostatic interactions between TPP and CS to some extent. At the same time, an endothermic peak at about 270 °C was found, indicating the breakdown of weak electrostatic interactions between α-galactosidase and CS. (Wan, Sun, & Li, 2009)

3.3. Encapsulation efficiency of α-galactosidase-loaded CS NPs

The CS and protein concentrations, ratio of CS/TPP, and MW of CS are normal factors usually discussed in protein-loaded NPs and other releasing systems. α-Galactosidase-loaded CS NPs were prepared as described in Section 2.2. The effects of various conditions, including CS and α-galactosidase concentrations, pH values, CS/TPP ratio, and CS MW, on α-galactosidase encapsulation efficiency were determined, the results of which are shown in Figs. 3–6. The means of the data were used to draw figures for this section.

3.3.1. Effects of concentration and pH of CS on encapsulation efficiency

As shown in Fig. 3, the encapsulation efficiency of α-galactosidase was affected by the concentration and pH of the CS solution. When the pH was increased from 4.0 to 5.5, the encapsulation efficiency of α-galactosidase gradually increased, finally decreasing when the pH reached 6.0. The encapsulation efficiency of α-galactosidase was also found to increase with increasing CS concentration from 1.0 mg/mL to 3.0 mg/mL at pH 5.5. α-Galactosidase-loaded CS NPs, however, were inclined to agglomerate at a CS concentration of 3.0 mg/mL.

In this work, pH was identified to be an important factor that significantly influences encapsulation efficiency. CS is a positive polymer in acidic solutions, and its positive potential decreases with increasing solution pH. The isoelectric point of α-galactosidase used in this study was 4.6 (Paloma, Leo, & Jaap, 1998). The positive potential of α-galactosidase decreased when the pH was increased from 3.0 to 4.5, after which the repellent force between CS and α-galactosidase weakened.

In contrast to the result where the positive potential of CS weakened when the pH value was increased from 5.0 to 6.0, the negative potential of α-galactosidase gradually became stronger. Thus, while the repulsive force between CS and α-galactosidase disappeared, the attraction between CS and α-galactosidase increased under the proper conditions. It appears that at pH 5.5, suitable inter- and intra-molecular linkages are created between TPP phosphates and the amino groups on C_2 of CS, such that the encapsulation efficiency of α-galactosidase increased.

3.3.2. Effects of CS/TPP ratios and pH of CS on encapsulation efficiency

The encapsulation efficiency of α-galactosidase in Fig. 4 shows that the maximum values of all the studied groups appeared at pH 5.5 when the CS/TPP weight ratios ranged from 8/1 to 3/1. In addition, the encapsulation efficiency of α-galactosidase increased when the CS/TPP ratios decreased from 8/1 to 3/1 at pH 5.5 (Fig. 4).

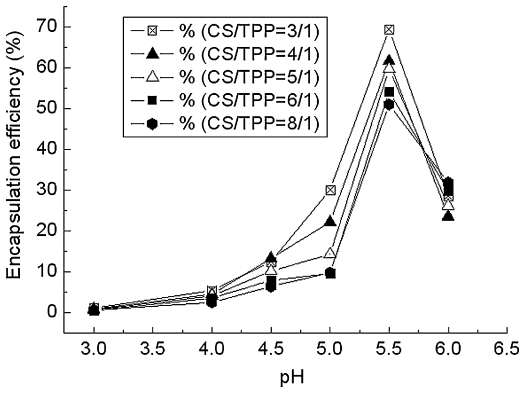

Fig. 4. Effects of CS/TPP ratios and pH on encapsulation efficiency.

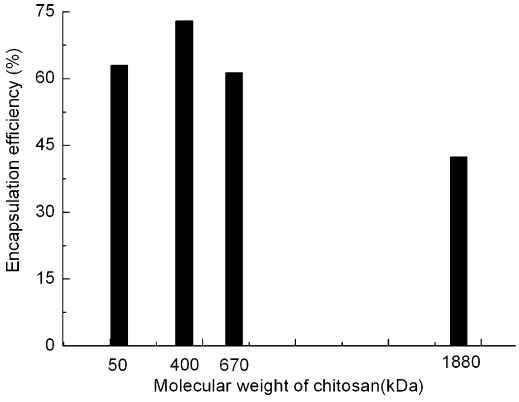

Fig. 6. Effects of CS MW on α-galactosidase encapsulation efficiency.

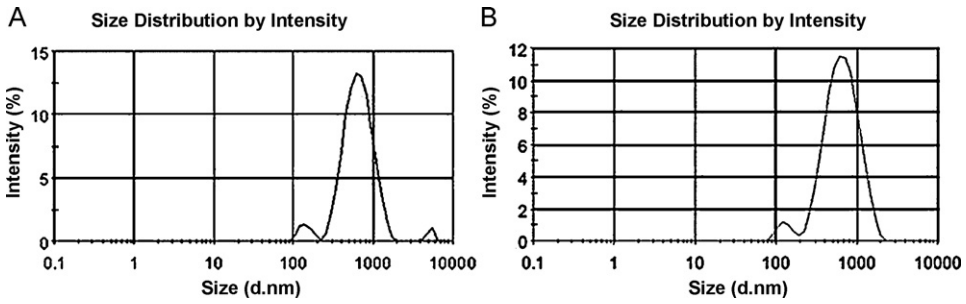

Fig. 7. Size distributions of CS and α-galactosidase-loaded CS NPs.

In order to produce high yields of stable and solid nanometric structures, the CS/TPP weight ratio should normally be within the range 3/1 to 6/1 (Bodmeier, Chen, & Paeratakul, 1989). In this work, however, stable CS NPs also appeared when the CS/TPP weight ratio was 8/1. This may be due to the diversity of purity, pH, and MW of CS employed. Consequently, the formulation parameters of CS NPs should be optimized for each individual CS type (Janes et al., 2001).

3.3.3. *Effects of α-galactosidase concentration on encapsulation efficiency*

Fig. 5 shows the encapsulation efficiency of α-galactosidase at various α-galactosidase concentrations. The encapsulation efficiencies were significantly affected by the final α-galactosidase concentration. The lower the α-galactosidase concentration was, the higher the encapsulation efficiency of α-galactosidase became. This effect could be attributed to competition between α-galactosidase and TPP in their interaction with CS. When the α-galactosidase concentration is low, the interaction between CS and TPP is strong. This suggests that ionically cross-linked CS/TPP NPs could be suitable for the higher encapsulation efficiency of α-galactosidase. Encapsulation efficiencies were higher than 60% when the final concentration of α-galactosidase was either less than or equal to 0.2 mg/mL, as shown in Fig. 5.

3.3.4. *Effects of CS MW on the encapsulation efficiency of α-galactosidase*

The effects of CS MWs (50, 400, 670, and 1880 kDa) on the encapsulation efficiency of α-galactosidase are shown in Fig. 6. α-Galactosidase-loaded CS NPs that used CS with an MW of 400 kDa showed the highest encapsulation efficiency, while those that used CS with an MW of 1880 kDa had the lowest. In addition, no significant differences in the encapsulation efficiencies of the NPs with CS MW of 50 and 670 kDa were observed.

3.4. *Physicochemical characterization of α-galactosidase-loaded CS NPs*

In order to illustrate the physicochemical characteristics of α-galactosidase-loaded CS NPs, their size distribution, surface charge, and morphology at pH 5.5 were analyzed using PCS, zeta potential analysis, and TEM, respectively. α-Galactosidase release profiles were also tested in this paper. Results are shown in Figs. 7–10.

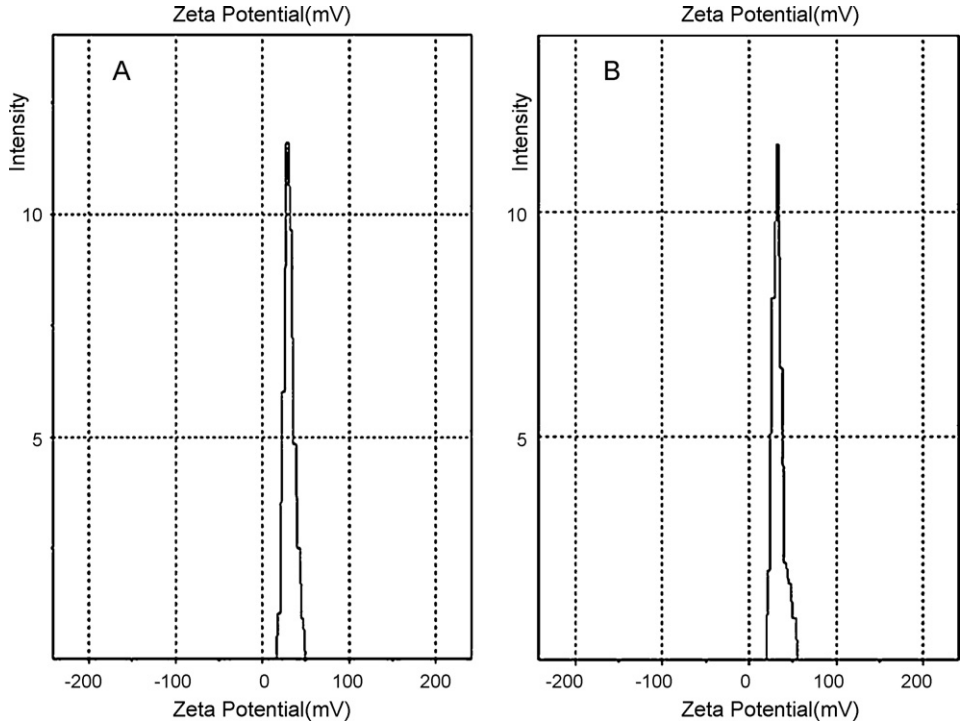

Fig. 8. Zeta potentials of CS NPs and α-galactosidase-loaded CS NPs.

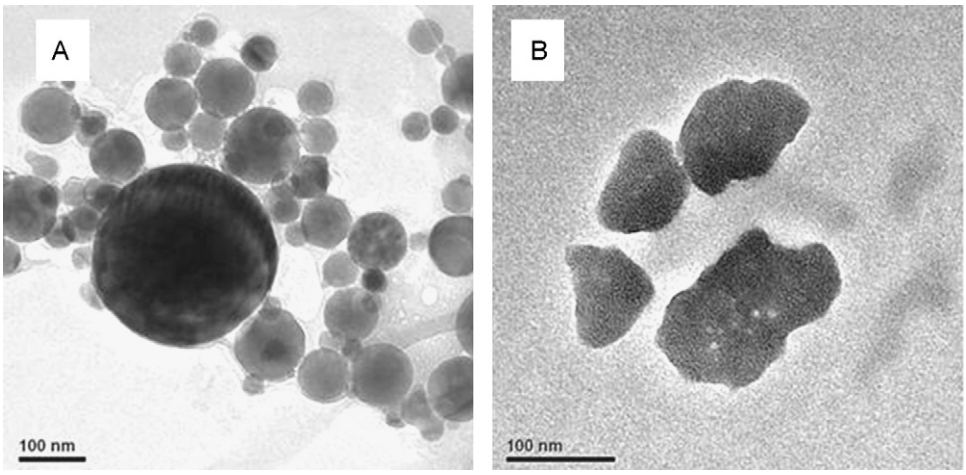

Fig. 9. TEM images of CS NPs and α-galactosidase-loaded CS NPs.

3.4.1. Size distribution of pure CS NPs and α-galactosidase-loaded CS NPs

Pure CS NPs featured polydisperse distributions with average particle sizes of 142.8, 698.8, and 5236 nm. According to PCS measurements, the volume fraction of the middle-sized particles (698.8 nm) was 93.9% (Fig. 7A). The particle size of 5236 nm was attributed to the aggregation of pure CS NPs with average particle sizes. After loading α-galactosidase, however, the size distribution changed into two peaks. The average particle sizes of α-galactosidase-loaded CS NPs became 132 nm and 715.6 nm. The volume fraction of the larger particles was 95.6% (Fig. 7B). The magnitude of the average particle sizes indicated the potential stability of the α-galactosidase-loaded CS NP system. α-Galactosidase-loaded CS NPs appeared to repel each other and there was dispersion stability. Hence, this system could be stable without aggregation, as there were no NP particle sizes larger than average.

3.4.2. Zeta potential analysis of pure CS NPs and α-galactosidase-loaded CS NPs

Fig. 8 shows the zeta potentials of both pure CS NPs and α-galactosidase-loaded CS NPs. All the measured zeta potential values were largely positive. The average zeta potential value for pure CS NPs was +28.5 mV (Fig. 8A), while that for α-galactosidase-loaded CS NPs was +31.5 mV (Fig. 8B). This is probably because the presence of positively charged CS on the surface of the NPs exerts some effects. At the same time, negatively charged α-galactosidase is encapsulated into the interiors of the NPs, but not on their shells. The magnitude of the zeta potential provides an indication of the possible stability of the nanoparticle system. All the nanoparticles had either negative or positive charges; they repelled each other, and there was dispersion stability. This system could be stable for more than 2 weeks without aggregation (Shu, Zhang, Teng, Wang, & Li, 2009). The zeta potential analysis shows that α-galactosidase-loaded CS NPs could be much more stable than pure CS NPs.

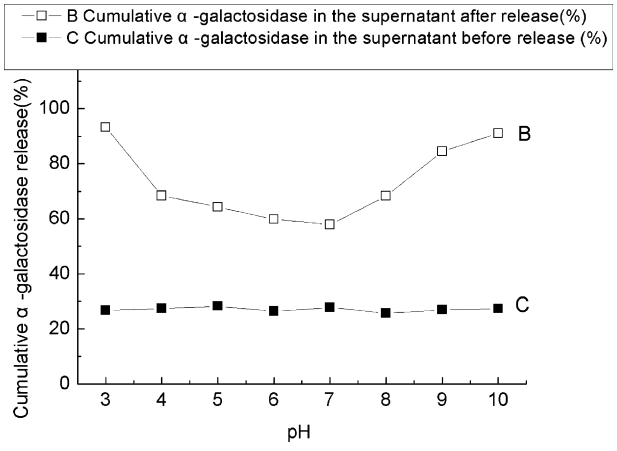

Fig. 10. Burst release ratio of α-galactosidase at different pH. Line B shows the cumulative α-galactosidase in the supernatant before release. Line C shows the cumulative α-galactosidase in the supernatant after treatment.

3.4.3. Morphology of pure CS NPs and α-galactosidase-loaded CS NPs

The morphology of pure CS NPs and α-galactosidase-loaded CS NPs were analyzed by TEM (Fig. 9). Pure CS NPs, possessed typical spherical shapes and smooth surfaces (Fig. 9A). In contrast, α-galactosidase-loaded CS NPs had largely irregular shapes (Fig. 9B). They also seemed to exhibit more compact structures than pure CS NPs. The differences in shape between pure CS NPs and α-galactosidase-loaded CS NPs may be explained by understanding that the formation of the latter is governed not only by electrostatic interactions between TPP and CS, but also between α-galactosidase and CS, the latter interaction being responsible for the controlled gelation of chitosan in a nanoparticulate form. This gelation and reticulation process may explain how the α-galactosidase-loaded CS NPs, acting as nanoresevoirs, were formed in this case and why the experimental NPs are more compact than pure CS NPs.

3.4.4. pH-mediated burst release of α-galactosidase

The burst release of α-galactosidase was influenced by the solution's pH (Fig. 10). The initial burst release, which occurred within 10 min, significantly depended on the pH of the buffer solution. The burst release percentage of α-galactosidase reached 90% when the solution's pH was either 3.0 or 10.0. However, the burst release of α-galactosidase was weakened visibly in the pH range between 3.0 and 10.0. Furthermore, nearly neutral solutions (pH 7.0) led to the lowest burst release of α-galactosidase, at which point it was less than 60%.

CS NPs are usually used for drug-controlled release, which features slow drug delivery over extended periods of time. However, feed enzymes for feed application require rapid release. For such applications, higher burst release efficiencies result in better feed enzyme effects. In this study, the significantly lower burst releases of α-galactosidase at pH 6.0 and 7.0 could be attributed to the slight breakage of α-galactosidase-loaded CS NPs and partial release of α-galactosidase from the NPs. Higher burst releases (over 90%) of α-galactosidase at pH 3.0 and 10.0, on the other hand, could be

due to the breaking of bonds between CS and TPP in strong acidic or alkaline solutions. Such conditions have the effect of eroding the polymer wall of the particles (Bai & Tien, 1999). In addition, pH conditions of 3.0 and 10.0 simulate the pH in the stomach and guts of pigs, in vitro. The burst release property could be useful in future requirements for controlled-release feed enzyme supplementation.

3.4.5. Thermal stability of α-galactosidase in α-galactosidase-loaded CS NPs

The residual activity of α-galactosidase in α-galactosidase-loaded CS NPs was 35.2%; in contrast, the residual activity of pure α-galactosidase was only 1.7%. The thermal stability of α-galactosidase was significantly enhanced after coating onto CS nanoparticles.

4. Conclusions

pH, CS MW, CS and α-galactosidase concentrations, and CS/TPP ratios had effect on encapsulation efficiency of α-galactosidase. It was found that the optimum conditions for the preparation of α-galactosidase-loaded CS NPs were as follows: a pH of 5.5, an initial CS concentration of 2 mg/mL, a final α-galactosidase concentration of 0.2 mg/mL, a CS/TPP ratio of 4/1, and a CS MW of 400 kDa. The pH of the solution appeared to significantly influence encapsulation efficiency. In addition, the thermal stability of α-galactosidase was significantly enhanced in the α-galactosidase-loaded CS NP system. The burst release of α-galactosidase seemed sensitive to the pH of the solution. With further improvement, this α-galactosidase-loaded CS NP system could be developed into a pH-sensitive feed enzyme-releasing system.

Acknowledgements

This work is supported by the Zhejiang Provincial Natural Science Foundation of China (Grant No. Y3090269) and the National Natural Science Foundation of China (Grant No. 50903026). The authors are thankful to the Zhejiang Academy of Agricultural Sciences for their financial support, the Zhejiang-California International Nano Systems Institute for the PCS tests, the Research Institute of Micro/Nano Science for the zeta potential tests, and the Instrumental Analysis Center of SJTU for the TEM analysis.

References

Amit, B., & Mika, S. (2009). Applications of chitin- and chitosan-derivatives for the detoxification of water and wastewater—A short review. *Advances in Colloid and Interface Science*, *152*(1–2), 26–38.

Ao, T., Cantor, A. H., Pescatore, A. J., Ford, M. J., & Pierce, J. L. (2004). In vitro and in vivo evaluation of simultaneous supplementation of α-galactosidase and citric acid on nutrient release, digestibility and growth performance of broiler chicks. *Poultry Science*, *83*(Suppl.), 148–1148.

Bai, R. B., & Tien, C. (1999). Particle deposition under unfavorable surface interactions. *Journal of Colloid and Interface Science*, *218*, 488–499.

Baucells, F., Perez, J. F., Morales, J., & Gasa, J. (2000). Effect of α-galactosidase supplementation of cereal-soya-bean-pea diets on the productive performances, digestibility and lower gut fermentation in growing and finishing pigs. *Journal of Animal Science*, *71*, 157–164.

Bautista, B. S., Hernandez, L. M., Bosquez, M. E., & Wilson, C. L. (2003). Effects of chitosan and plant extracts on growth of colletotrichum gloeosporioides, anthracnose levels and quality of papaya fruit. *Crop Protection*, *22*(9), 1087–1092.

Bodmeier, R., Chen, H. G., & Paeratakul, O. (1989). A novel approach to the oral delivery of micro- or nanoparticles. *Pharmaceutical Research*, *6*(5), 413–417.

Cagri, A., Ustunol, Z., & Ryser, E. T. (2004). Antimicrobial edible films and coatings. *Journal of Food Protection*, *67*(4), 833–848.

Fu, J. H., Ji, J., Yuan, W. Y., & Shen, J. C. (2005). Construction of antiadhesive and antibacterial multilayer films via layer-by-layer assembly of heparin and chitosan. *Biomaterials*, *26*(33), 6684–6692.

Irma, F. d. H., Ana, M. M. R., Caren, M. V. Z., Peter, J. P., & Cees, A. M. J. J. V. D. H. (1992). Cloning and expression of a member of the Aspergillus niger gene family encoding a-galaetosidase. *Molecular and General Genetics*, *233*, 404–410.

Janes, K. A., Calvo, P., & Alonso, M. J. (2001). Polysaccharide colloidal particles as delivery systems for macromolecules. *Advanced Drug Delivery Reviews*, *47*, 83–97.

Jayakumara, R., Prabaharanb, M., Naira, S. V., & Tamura, H. (2010). Novel chitin and chitosan nanofibers in biomedical applications. *Biotechnology Advances*, *28*(1), 142–150.

Khalid, M. N., Agnely, F., Yagoubi, N., Grossiord, J. L., & Couarraze, G. (2002). Water state characterization, swelling behavior, thermal and mechanical properties of chitosan based networks. *European Journal of Pharmaceutical Sciences*, *15*(5), 425–432.

Kidd, M. T., Morgan, G. W., Jr., Zumwalt, C. D., Price, C. J., Welch, P. A., Brinkhaus, F. L., et al. (2001). α-Galactosidase enzyme supplementation to corn and soybean meal broiler diets. *Journal of Applied Poultry Research*, *10*, 186–193.

Kim, S. W. (2002). Effect of alpha-1,6-galactosidase, beta-1,4-mannanase and beta-1,4-mannosidase on intestinal morphology and the removal of dietary antinutritional factors in young pigs. *Journal of Animal Science*, *80*(Suppl. 1), 39 (Abstract).

Kittur, F. S., Harish Prashanth, K. V., Udaya Sankar, K., & Tharanathan, R. N. (2002). Characterization of chitin, chitosan and carboxymethyl derivatives by differential scanning colorimetry. *Carbohydrate Polymer*, *49*, 185–193.

Knaul, J. Z., Hudson, S. M., & Creber, K. A. M. (1999). Improved mechanical properties of chitosan fibers. *Journal of Applied Polymer Science*, *72*, 1721–1731.

Kobayashi, S., Terashima, Y., & Itoh, H. (2002). Effects of dietary chitosan on fat deposition and lipase activity in digesta in broiler chickens. *British Poultry Science*, *43*(2), 270–273.

Li, J., Liu, Q., Liu, Y. J., Liu, S. C., & Yao, S. Z. (2005). DNA biosensor based on chitosan film doped with carbon nanotubes. *Analytical Biochemistry*, *346*(1), 107–114.

Masotti, A., & Ortaggi, G. (2009). Chitosan micro- and nanospheres: Fabrication and applications for drug and DNA delivery. *Mini-Reviews in Medicinal Chemistry*, *9*(4), 463–469.

Mi, F. L., Shyu, S. S., Wu, Y. B., Lee, S. T., Shyong, J. Y., & Huang, R. N. (2001). Fabrication and characterization of a sponge-like asymmetric chitosan membrane as a wound dressing. *Biomaterials*, *22*(2), 165–173.

Paloma, M., Leo, H. D. G., & Jaap, V. (1998). Characterization of galactosidases from Aspergillus niger: Purification of a novel α-galactosidase activity. *Enzyme and Microbial Technology*, *22*, 383–390.

Pittler, M. H., & Ernst, E. (2004). Dietary supplements for body-weight reduction: A systematic review. *American Journal of Clinical Nutrition*, *79*(4), 529–536.

Qi, L. F., Xu, Z. R., Xia, J., Hu, C. H., & Zou, X. F. (2004). Preparation and antibacterial activity of chitosan nanoparticles. *Carbohydrate Research*, *339*, 2693–2700.

Senel, S., & Susan, J. M. (2004). Potential application of chitosan in veterinary medicine. *Advanced Drug Delivery Reviews*, *56*, 1467–1480.

Shu, S. J., Zhang, X. G., Teng, D. Y., Wang, Z., & Li, C. X. (2009). Polyelectrolyte nanoparticles based on water-soluble chitosan–poly (L-aspartic acid)–polyethylene glycol for controlled protein release. *Carbohydrate Research*, *344*, 1197–1204.

Wan, A. J., Sun, Y., & Li, H. L. (2009). Characterization of novel quaternary chitosan derivative nanoparticles loaded with protein. *Journal of Applied Polymer Science*, *114*(5), 2639–2647.

Wang, Y. C., Lin, M. C., Wang, D. M., & Hsieh, H. J. (2003). Fabrication of a novel porous PGA-chitosan hybrid matrix for tissue engineering. *Biomaterials*, *24*(6), 1047–1057.

Xu, Y. X., Li, Y. L., Liu, Y., Xu, S. C., & Yao, X. H. (2009). Purification and characterization of α-galactosidase from Aspergillus niger v. Tiegh RM48. *Journal of Zhejiang University (Agriculture and Life Sciences)*, *2*, 147–152.